Modern Environmental Science and Engineering (ISSN 2333-2581)
January 2020, Volume 6, No. 1, pp. 84-98
Doi: 10.15341/mese(2333-2581)/01.06.2020/007
Academic Star Publishing Company, 2020
www.academicstar.us

Five-day Cycle of the Surface Wind in the Alcântara Launch Center During the Dry Quarter

Karlos André Câmara Ramalho[1,3], and Marcos Daisuke Oyama[2]

1. Instituto Nacional de Pesquisas Espaciais, Centro de Previsão de Tempo de Estudos Climáticos, Cachoeira Paulista, SP, Brazil

2. Instituto de Aeronáutica e Espaço, Divisão de Aerodinâmica, Controle e Estruturas, São José dos Campos, SP, Brazil

3. Departamento de Controle do Espaço Aéreo, Centro Integrado de Meteorologia Aeronáutica, Rio de Janeiro, RJ, Brazil

Abstract: The Alcântara Launch Center (Centro de Lançamento de Alcântara, CLA) is the main launch site for the Brazilian aerospace vehicles and located on the northern coast of Northeast Brazil. The 5-day cycle (C5d) is a variability in the 3-9 days band that is found in the surface wind data at CLA during the dry quarter (September to November). This study aimed to characterize C5d and find out the main atmospheric factors related to the C5d phases, VMAX (VMIN), which contains the more intense (weaker) winds. Surface wind data measured at CLA and ERA-Interim reanalysis data for the dry quarter over the course of 9 years – 1996-1999, 2005, 2012-2015 – were used. Wavelet transform was applied to the observed data to obtain C5d features, while reanalysis data for a number of cases were used to obtain the average large-scale factors related to C5d phases. Results showed that C5d period is concentrated around 5 days, C5d occurs frequently and its active periods occur in about 1/3 of dry quarter days. The distribution of wind speed and direction for C5d phases showed that, from VMAX to VMIN, the surface wind over CLA weakens (reduction from 9-12 m/s to 9-6 m/s) and rotates counterclockwise (from ENE to NE direction). To obtain the distinct features between the C5d phases, 35 cases that represent typical cases of C5d during active periods were analyzed. Results showed that, from VMAX to VMIN, the South Atlantic Subtropical High (SASH) weakens or propagates eastwards for all cases, while the North Atlantic Subtropical High (NASH) weakens or propagates northwards for about 3/4 of cases. Therefore, SASH could be regarded as the main driver of C5d, while NASH could be considered as an important complementary forcing of C5d.

Key words: Alcântara Launch Center, C5d, surface wind

1. Introduction

The Alcântara Launch Center (*Centro de Lançamento de Alcântara*, CLA) is the main launch site for the Brazilian aerospace vehicles[1]. It is located on the northern coast of Northeast Brazil (NEB), in the city of Alcântara, state of Maranhão (Fig. 1). The geographical position of CLA near the Equator is favorable for launching geosynchronous satellites. The climate in CLA is tropical humid, with high monthly temperatures throughout the year (26-28°C) and annual precipitation (~1800 mm) distributed over the seasons with higher totals (~1000 mm) in austral autumn (wet quarter, March to May, MAM) and lower (< 50 mm) in austral spring (dry quarter, September to November, SON) [1, 2].

Particular environmental conditions, such as the absence of precipitation, lightning and strong surface winds, are necessary for the successful launch of Brazilian aerospace vehicles at CLA (Marques and Fisch 2005). During the dry quarter, the limiting factor for launch at CLA is usually the presence of strong surface winds, because the average surface wind speed is higher [1, 3] and precipitation events are infrequent [2, 4]. Wind speed is an important factor because it affects the flight trajectory of aerospace vehicles [5].

Corresponding author: Marcos Daisuke Oyama, Ph.D., research areas/interests: tropical Meteorology, wind, precipitation. E-mail: marcos.oyama@ymail.com.

[1] http://www.aeb.gov.br/programa-espacial-brasileiro/infraestrutura-de-solo/centros-de-lancamento/.

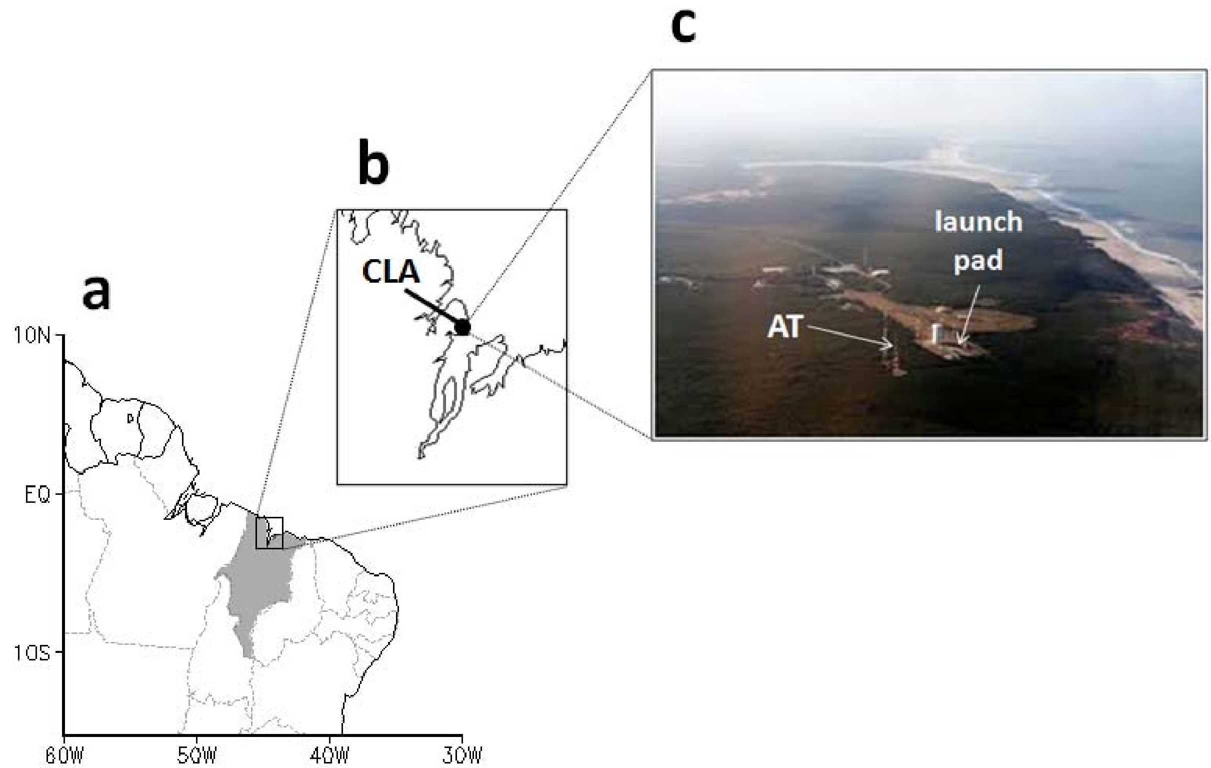

Fig. 1 (a) The boundaries of Brazilian states are indicated by gray dotted lines. The state of Maranhão is shaded in gray. (b) The box-like region that includes CLA is zoomed in and the approximately location of CLA is shown. (c) The position of the launch pad and the anemometric tower (AT) are indicated on the aerial view of CLA. Average winds blow from the ocean to AT.

Numerous studies have addressed the wind characteristics at CLA. They include the computation of climatological means [1, 3], the characterization of surface and internal boundary layers [6], the numerical simulation of rocket exhaust clouds dispersion [7] and the wind-tunnel simulation of the surface flow over CLA [8]. For short-range weather forecasting (12 h to 3 days), Silva and Fisch (2014) [9] showed that simulations using the Weather Research and Forecasting model (WRF) driven by forecasts from the Global Forecast System (GFS) were able to suitably represent the observed wind profiles at CLA during periods of the wet and dry quarters. Souza (2014) [10] reported that simulations of this kind were useful to define the launch time during the operation at CLA called *Operação Raposa* (12-Aug to 03-Sep-2014). A comparison between the observed and simulated surface wind during this operation was carried out by Custódio et al. (2017) [11].

Although numerical modeling has a promising potential for wind forecasting, there is still a research gap in understanding the surface wind signal variability at scales relevant to short-range weather forecasting. One such variability is a cycle with periodicity in the 3-9 days band that is found in the surface wind speed data at CLA during the dry quarter. This cycle, hereafter referred to as 5-day cycle (C5d), because its average periodicity is about 5 days, can be split in phase of maximum wind speed (VMAX), which contains the more intense winds, and phase of minimum wind speed (VMIN), which contains the weaker winds and is thus more suitable for launch of aerospace vehicles. C5d had been noticed by meteorologists who participated in launch operations at

CLA and used empirically by them to assist the surface wind forecasting [12]. The existence of C5d was also suggested by results from a field campaign called "Murici-2" (Sep-2008): Marciotto et al. (2012) [13] found 4-day cycle in wind speed at 10 m and Reuter (2013) [14] found a similar cycle in surface pressure measured by a microbarograph.

The presence of C5d (or cycles similar to C5d) has also been reported for several regions around the world [15-17] and, in particular, for a locality in the eastern coast of NEB (Marechal Deodoro, state of Alagoas, Brazil; [18]). These studies suggest, in general, that this cycle could be driven by atmospheric systems whose variability lies in the 3-9 days band, such as transient synoptic systems in middle-latitudes and easterly wave disturbances in low-latitudes. Diedhiou et al. (2010) [19] showed that easterly wave disturbances can propagate across the Atlantic Ocean towards NEB and mainly affect its eastern coast [20]. Frontal systems initiated from middle-latitude transient synoptic waves in the Southern Hemisphere propagate southwesterly over South America and can also affect NEB [21], particularly its southern part [22]. Therefore, C5d in NEB could be directly related to both systems.

Easterly waves or frontal systems affect CLA, but it is not located in the main areas influenced by them. Coutinho and Fisch (2007) [23] and Marques et al. (2009) [24] showed that easterly waves affect CLA all year round, with higher occurrence in July. Marques (2004) [25] and Tavares (2008) [26] studied frontal systems cases which affect the weather conditions (including the surface wind) at CLA. Although these studies suggest a possible relation between C5d in CLA and easterly waves or frontal systems, there are important aspects that do not fit into this relationship. For instance, easterly waves affect higher levels (above 850 hPa) and are hardly detectable in the surface wind signal [24], and only intense and infrequent frontal systems are able to affect CLA [26]. These features do not agree with the fact that C5d can be clearly identified in the surface wind signal [13] and is relatively frequent during the dry quarter (according to empirical knowledge).

To contribute to the clarification of the above mentioned issues, the present study focus on C5d in CLA during the dry quarter and aims to 1) characterize C5d and 2) find out the main atmospheric factors related to the C5d phases (VMAX and VMIN). The first objective includes the application of wavelet transform (WT; [27]) on surface wind data collected at CLA and expanding the C5d identification found in previous works [13] by using a longer dataset. The second objective consists of providing a reasonable explanation about C5d phases, because those based on the occurrence of easterly waves [24] or frontal systems [26] have severe limitations. To achieve this objective, reanalysis data for a number of cases are used to obtain the average large-scale factors related to C5d phases.

The study is organized as follows. In section 2, observed and reanalysis data are described and the use of WT is explained. Results are given in sections 3 (observed features of C5d), 4 (case studies to illustrate the main large-scale factors related to C5d phases) and 5 (distinct features between the C5d phases). Results are integrated and discussed in section 6 and concluding remarks are provided in section 7.

2. Data and Methods

Observed surface wind data (wind speed and direction) for the dry quarter (SON) over the course of 9 years — 1996-1999, 2005, 2012-2015 — are used. Measurements are made by an aerovane installed in the sixth level (70 m from the ground) of the anemometric tower located close to the launch pad at CLA (Fig. 1c) (see [28] for details). The measurement frequency is 0.5 Hz and 10-min statistics are stored in a datalogger. The 10-min averages are aggregated to produce the hourly time series of surface wind data. Then, moving average is applied in the time series to filter out the daily cycle.

Zonal and meridional wind at 1000 hPa and sea level pressure (SLP) from the ERA-Interim dataset [29], for the same period of the observed data, are used. Reanalysis data is available over a global 0.75° × 0.75° grid at four analysis times (0000, 0600, 1200 and 1800 UTC). Daily fields are computed as the mean of these four times.

To identify C5d, WT [27] is applied to the normalized and detrended time series of wind speed for the dry quarter of each year. The Morlet wavelet (periodic function in time modulated by a Gaussian function) is used as the basis function. The level of statistical significance is prescribed as 95%.

The full WT output (using the software provided by Torrence and Compo [27] for a single year (dry quarter of 1999) is illustrated in Fig. 2. Given the normalized and detrended time series of wind speed — called input time series (Fig. 2a) — the WT decomposes the signal in time and scale (period), and results in the wavelet power spectrum (Fig. 2b). It shows the time intervals when higher power values within a band (scale interval) of interest are found.

For each scale, the time average of the wavelet power produces the global wavelet spectrum (Fig. 2c), which is equivalent to the Fourier transform spectrum. The signal variability is concentrated on scales at which power peaks (relative maxima) occur in the global wavelet spectrum.

The average within a band of interest results in the time series of the scale-averaged wavelet power (SAWP; Fig. 2d). SAWP is a non-negative number that measures the activity of the band-related variability. Time intervals when SAWP is higher, i.e., above a prescribed threshold, are called active periods.

The WT is also used to filter the signal by removing (retaining) all variabilities on scales outside (inside) the band of interest. This reconstructed signal is called filtered time series.

For C5d, the band interval and SAWP thresholds are prescribed as follows.

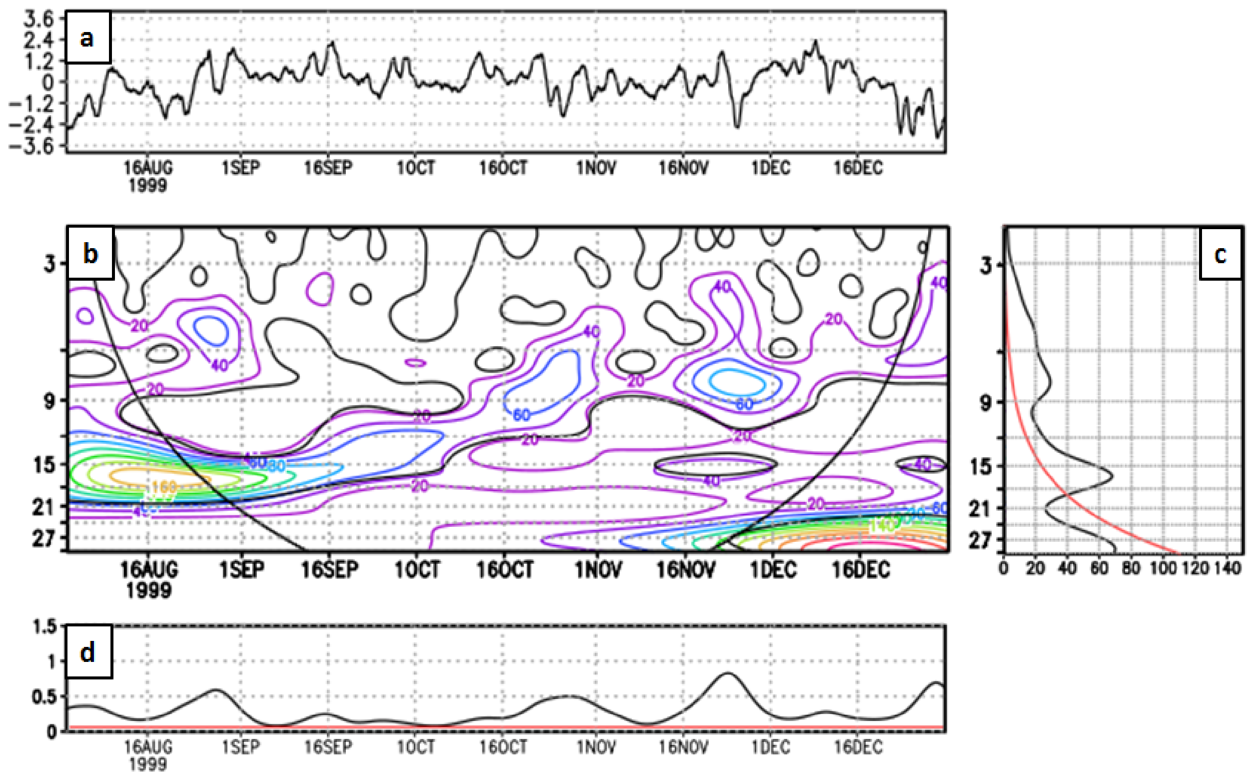

Fig. 2 Illustration of the WT output for the dry quarter of 1999: (a) input time series, (b) wavelet power spectrum, (c) global wavelet spectrum and (d) time series of SAWP in the 3-9 days band. Statistically significant values at 95% are enclosed by black lines in panel b and above the red line in panels c and d.

- The broader 3-9 days band is assumed as the band of interest. This band is used for computation of SAWP and obtaining the filtered time series.
- Occurrence of C5d means SAWP > the threshold for statistical significance at 95%.
- Active period of C5d means SAWP > 0.4.

These assumptions are addressed in the section 3 and their application can be illustrated by analyzing Fig. 2. For the dry quarter of 1999, the power peak at ~7 days in the 3-9 days band corresponds to C5d period (Fig. 2c). C5d occurs quite frequently, because SAWP is significant most of time, but C5d active periods (SAWP > 0.4) are restricted to two periods in SON: second half of October and second half of November (Fig. 2d).

3. Observed Features of C5d

The global wavelet spectrum for the dry quarter (SON) of each year, obtained from the observed wind data, is shown in Fig. 3. In most years, the 3-9 days band lies between two relative minima of power (one minimum below 3 days and the other between 9 and 12 days) and shows one or two relative maxima of power within the band. Therefore, C5d is suitably delimited by the assumed band limits at 3 and 9 days (section 2).

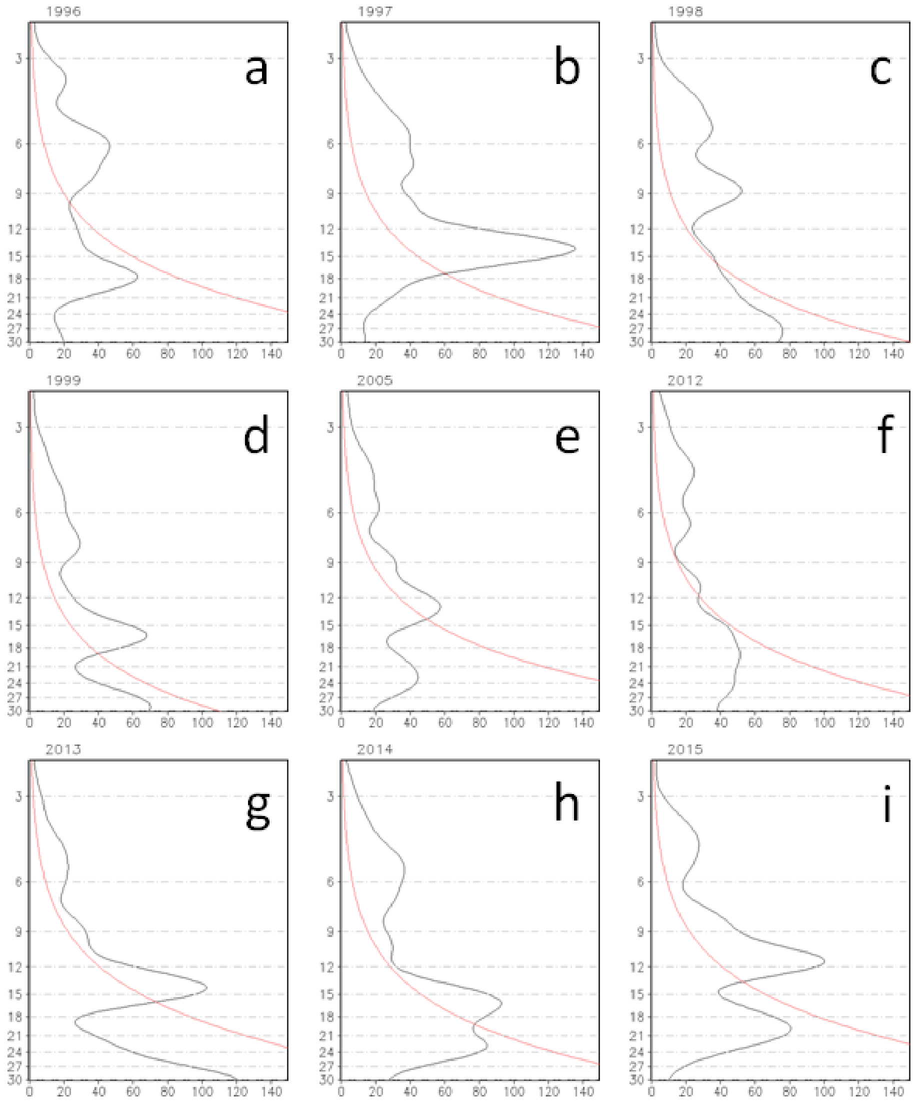

Fig. 3 Global wavelet spectrum for the dry quarter of each year: (a) 1996, (b) 1997, (c) 1998, (d) 1999, (e) 2005, (f) 2012, (g) 2013, (h) 2014 and (i) 2015.

In the 3-9 days band, there are significant peaks about 5 days and, in about half of years, two significant peaks (1996, 1997, 1998, 2012). Power values in the peaks show marked interannual variability. Outside the 3-9 days band, significant peaks also occur around 15 days (e.g., 1997) and non-significant peaks around 22 days (e.g., 2015), but they are beyond the scope of this study.

To obtain the period around which the variability in the 3-9 days band is concentrated, the cumulative frequency distribution of periods related to power peaks (in global wavelet spectra in Fig. 3) within the 3-9 days band is shown in Fig. 4. The mode occurs between 5 and 6 days, and the median corresponds to the period of 5.4 days. This result justifies the use of the term "5-day cycle" for this variability and ratifies the periodicity identified by previous studies from more limited data [12, 13].

Statistically significant values of SAWP (≥ 0.06 to 0.35 depending on the year) indicate C5d occurrence. However, to select the active periods of C5d, i.e., the time intervals when C5d dominates the wind speed signal, a more restrictive threshold of SAWP, 0.4, is assumed (section 2). It is obtained subjectively by comparing the input with the filtered time series. For instance, for the dry quarter of 1996 (Fig. 5), when SAWP > 0.4, both series show similar high values of

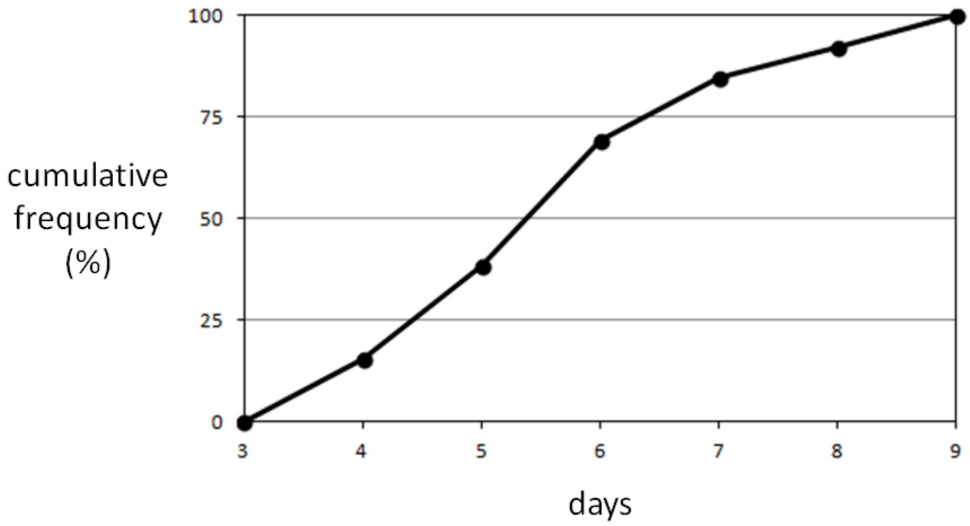

Fig. 4 Cumulative frequency distribution of periods related to the power peaks within the 3-9 days band found in the global wavelet spectra shown in Fig. 3.

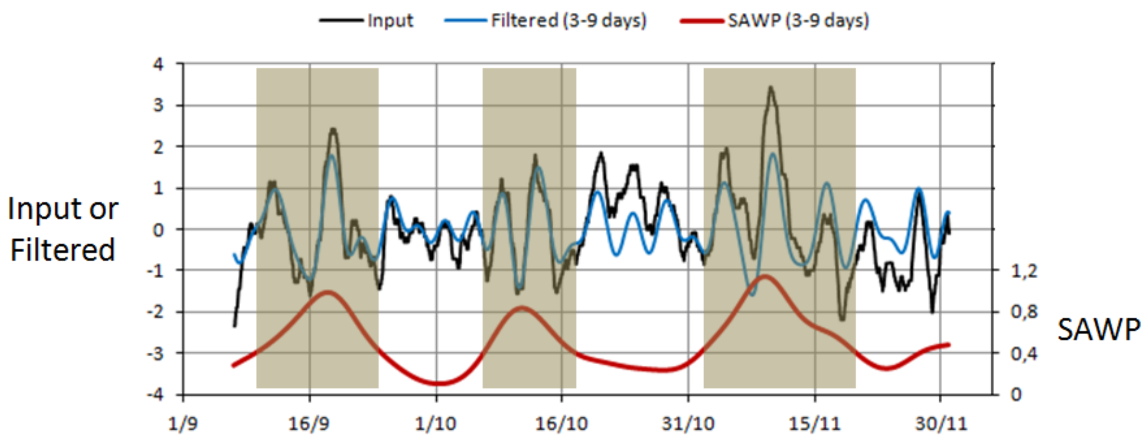

Fig. 5 Input (black line), filtered (blue) and SAWP (red) time series for the dry quarter of 1996. Filtered and SAWP time series refer to the 3-9 days band. Time intervals when SAWP > 0,4 (active periods) are shaded.

amplitude. For lower values of SAWP, eventual moderate/high amplitudes in the input time series may not be related to C5d: for instance, the moderate wind speed drop between 21 and 23-Nov in the input time series is greatly smoothed in the filtered time series. The threshold value of 0.4 is similar to that used by Souza and Oyama (2017) [29] for breeze potential occurrence.

For each year, the fraction of dry quarter days in which there is occurrence or active period of C5d is shown in Fig. 6. On average, C5d occurs in 85% of dry quarter days. It ratifies the empirical knowledge (from meteorologists who participated in launch operations at CLA) that C5d is relatively frequent. C5d active periods correspond, on average, to 28% of dry quarter days. This fraction is expressive, because it corresponds to about 1/3 of the dry quarter, and explains the usefulness of the method of empirically adjusting a periodic function to the daily surface wind data for short-range forecasting purposes [12]. The smallest fraction of days in active periods (about 10%) occurred in 2005, which is consistent with the less pronounced peak in the 3-9-days band for this year (Fig. 3e).

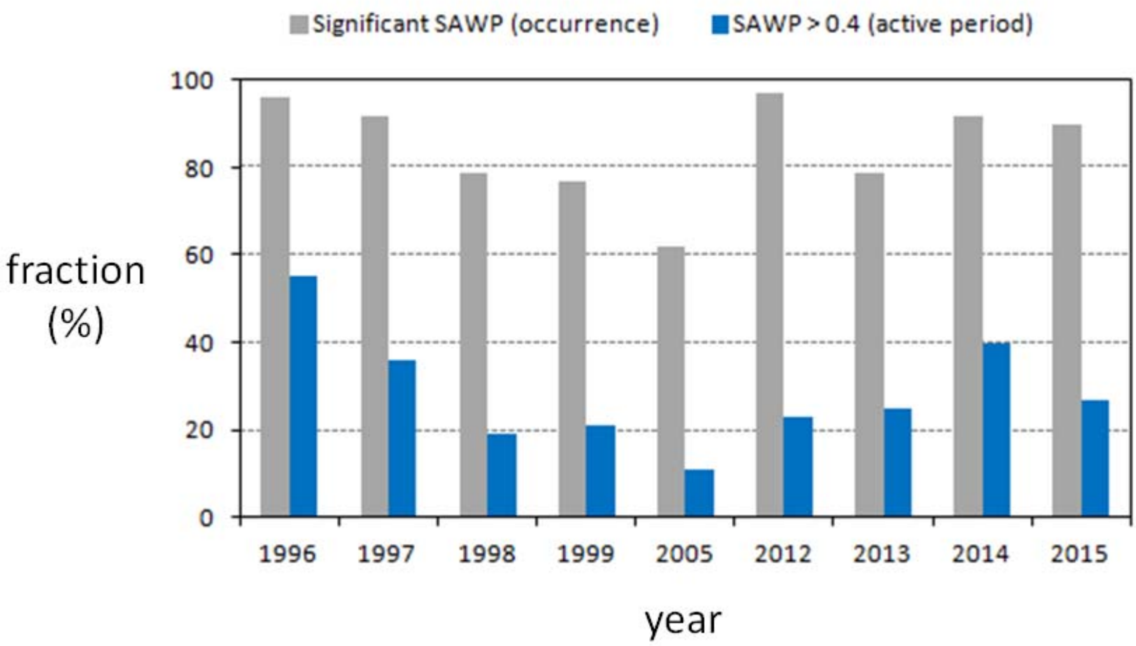

Fig. 6 Fraction of dry quarter days for each year in which there is occurrence (gray bar) or active period (blue bar) of C5d.

The distribution of wind speed and direction for C5d phases is shown in Fig. 7. In VMIN, higher frequency is found in ENE (40%) and NE (44%) directions, and wind speed is 6-9 m/s. These features are similar to those found for the whole dry quarter [3, 30]. In VMAX, the highest frequency is found in ENE (60%) direction and wind speed increases to 9-12 m/s. Therefore, from VMAX to VMIN, the surface wind over CLA weakens (reduction of about 3 m/s) and rotates counterclockwise (from ENE to NE direction).

The characterization of C5d is also carried out using the ERA-Interim reanalysis data for the grid point closest to CLA. For all years, there is a good agreement of periods of C5d activity between observed and reanalysis data [31]. For instance, a comparison of SAWP computed from both datasets for two contrasting years, 1996 and 1999, is shown in Fig. 8. In 1996, when there are more days in C5d active periods (Fig. 6), the timing of observed peaks is well represented by reanalysis data, although the observed power is underestimated in the first two peaks. In 1999,

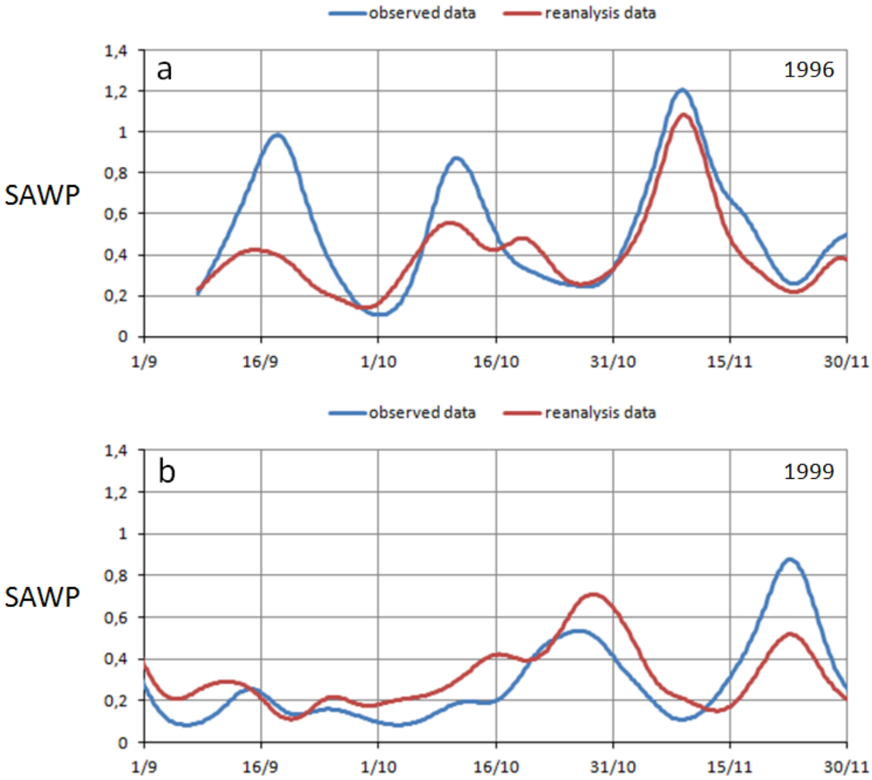

Fig. 7 Distribution of wind speed and direction for C5d phases: (a) VMAX and (b) VMIN.

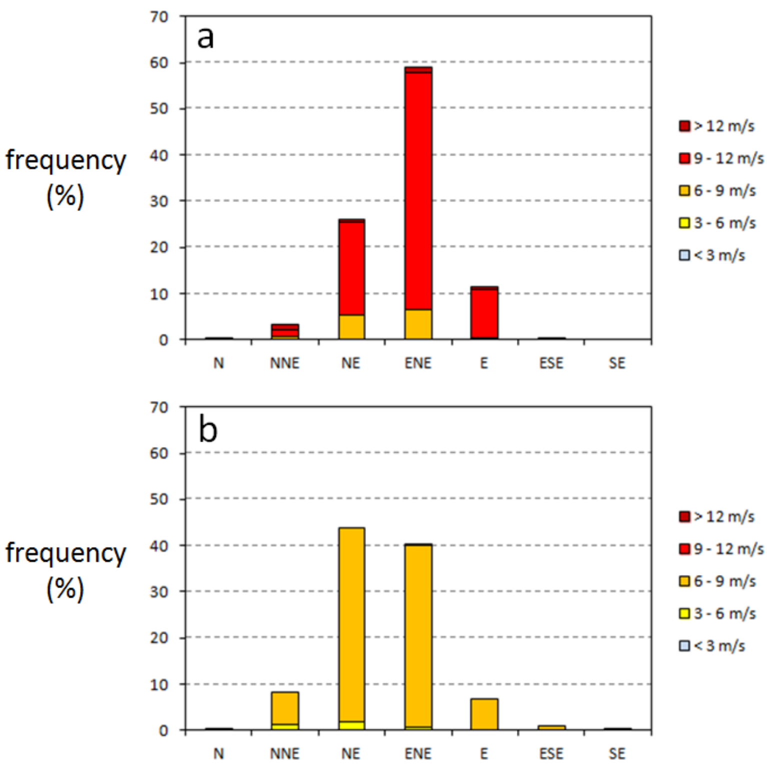

Fig. 8 Time series of SAWP computed from observed (blue) and reanalysis (red) data for the dry quarter of 1996 (a) and 1999 (b).

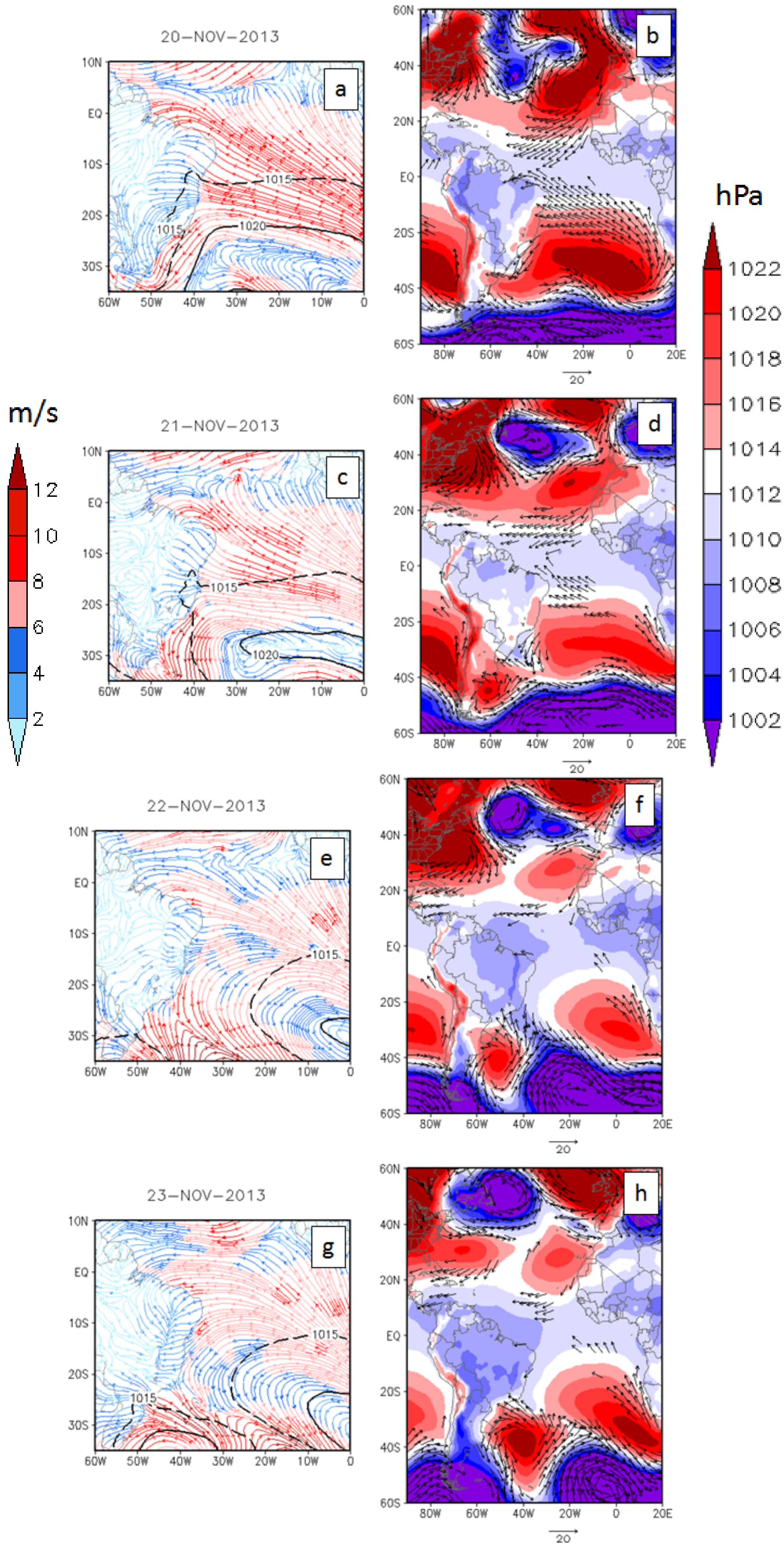

Fig. 9 Atmospheric circulation at 1000 hPa and SLP: 20 (a, b), 21 (c, d), 22 (e, f) and 23-Nov-1999 (g, h). Panels a, c, g: streamlines with wind speed (left color bar); two isobars are also plotted (continuous and dashed back lines). Panels b, d, f, h: SLP is shaded (right color bar) and wind vectors with magnitude above 8 m/s are plotted.

when there are less days in C5d active periods (Fig. 6), reanalysis data is able to reproduce the observed lack of C5d activity in the first half of the dry quarter. For all years, C5d features — global wavelet spectrum in the 3-9 days band, median of periods related to power peaks and distribution of wind speed and direction for C5d phases — are similar for both datasets (Ramalho 2018).

4. CaseStudies

In this section, 3 cases in active periods of C5d are briefly analyzed to illustrate the main large-scale factors related to C5d phases.

The first case occurred from 20 to 23-Nov-2013 and illustrates the transition from VMAX to VMIN (Fig. 9). In both phases, southeast trades from the northern border of the South Atlantic Subtropical High (SASH; [32]), after crossing the ocean, undergoes a counterclockwise rotation over the northern coast of NEB (where CLA is located).

- In 20-Nov (VMAX), more intense southeast trades occur over a large area that includes the South Atlantic and the eastern and northern coast of NEB. SASH is intense and extends over the entire South Atlantic.
- From 21 to 23-Nov (VMIN), southeast trades weaken and the area with higher wind velocities shrinks and disappears. The counterclockwise rotation over the northern coast of NEB becomes more pronounced, which agrees with the higher frequency in the NE direction for VMIN mentioned in section 3 (Fig. 7b). SASH weakens and is pushed eastward by the northward propagation of the trough and the migratory anticyclone (behind the trough) associated to a frontal system affecting Southern Brazil [33].

Therefore, for this case, the transition between C5d phases is explained by changes in the intensity of southeast trades that are related to changes in SASH features (intensity and zonal position) driven by the passage of a cold front in Southern Brazil.

- The other two cases — 10-Nov-1996 and 12-Sep-2013 — illustrate the influence of the North Atlantic Subtropical High (NASH; [34]) on C5d phases (Fig. 10), because NASH also influence the intensity of southeast trades winds [35]. For both cases, SASH features are similar to those of 20-Nov-1996; therefore, conditions in South Atlantic are favorable to the establishment of VMAX.
- In 10-Nov-1996, NASH is intense and displaced to the south, and these conditions intensify northeast trades over the North Atlantic. Combined the intense southeast trades from SASH, the result is a large continuous area with intense winds in both Hemispheres that advances inland over NEB. This area is much larger than that of 20-Nov-1996. This leads to the establishment of an unambiguous VMAX.
- In 12-Sep-2013, Hurricane Humberto is found at about 20°N [36]. It pushes NASH northwards and northeast trades become confined to higher latitudes of the Northern Hemisphere. The hurricane also acts as a sink of southeast trades and shifts the southeasterly circulation over the ocean in 10°S-Equator slightly eastward. It reduces the wind speed over the northern coast of NEB and leads to the establishment of VMIN, contrary to the expected from conditions in South Atlantic.

These results confirm that NASH features (intensity and meridional position) could also affect southeast trades and, therefore, C5d phases.

5. Features of C5d Phases

To obtain the distinct features between the C5d phases, the following procedure is carried out for 35 cases (on average, about 4 cases per year) that represent typical cases of C5d during active periods. Sampling

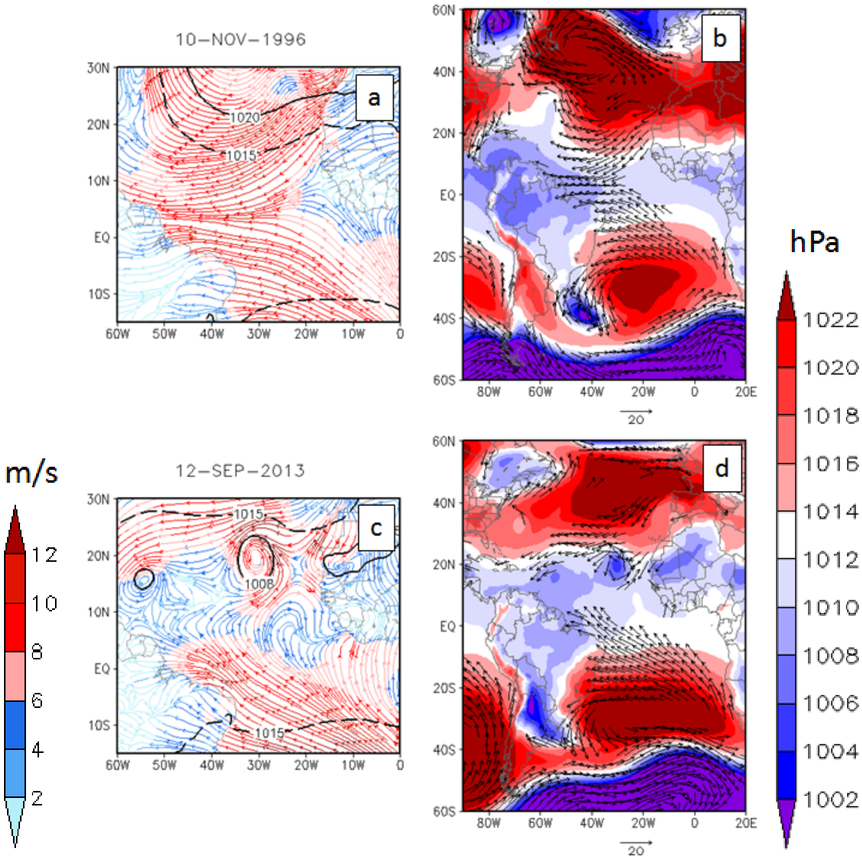

Fig. 10 Atmospheric circulation at 1000 hPa and SLP: 10-Nov-1996 (a, b) and 12-Sep-2013 (c, d). Panels a, c: streamlines with wind speed (left color bar); two isobars are also plotted (continuous and dashed back lines). Panels b, d: SLP is shaded (right color bar) and wind vectors with magnitude above 8 m/s are plotted.

criteria include the clear (unambiguous) presence of C5d phases in the input time series of both observed and reanalysis data. For a given case, from VMAX to VMIN, changes in three features of SASH are subjectively identified:

- intensity: intensification (+), no change (0) or weakening (–);
- zonal position: eastward displacement (E), no change (0) or westward displacement (W); and
- meridional position: northward displacement (N), no change (0) or southward displacement (S).

The same procedure is carried out for NASH. Frequencies for each category are shown in Fig. 11.

The transition from VMAX to VMIN is generally related to weakening of SASH and NASH (74% and 49% of cases, respectively), eastward displacement of SASH (86%) and northward displacement of NASH (60%). These features agree with those found in section 4. Meridional displacement of SASH or zonal displacement of NASH is not found for the majority of cases (69% and 97%, respectively). Westward displacement of SASH does not occur for all cases. These results motivate defining, in the transition from VMAX to VMIN, the "influence" of SASH when it weakens or propagates eastwards, and the "influence" of NASH when it weakens or propagates northwards. The frequencies of "influence" defined in this way are also shown in Fig. 11.

For all cases ("YES" in Fig. 11a), there is influence of SASH. This is an important and robust result, because it shows a common feature for all cases: VMAX (VMIN) is related to higher (lower) intensity of SASH or more (less) zonal proximity of SASH to South America. Therefore, SASH can be regarded the main forcing of C5d.

For the majority of cases (74%; “YES” in Fig. 11b), there is influence of NASH. This is also an important result, because for about 3/4 of cases VMAX (VMIN) is related to higher (lower) intensity of NASH or more (less) meridional proximity of NASH to the Equator. Therefore, NASH can be regarded as an important complementary forcing of C5d.

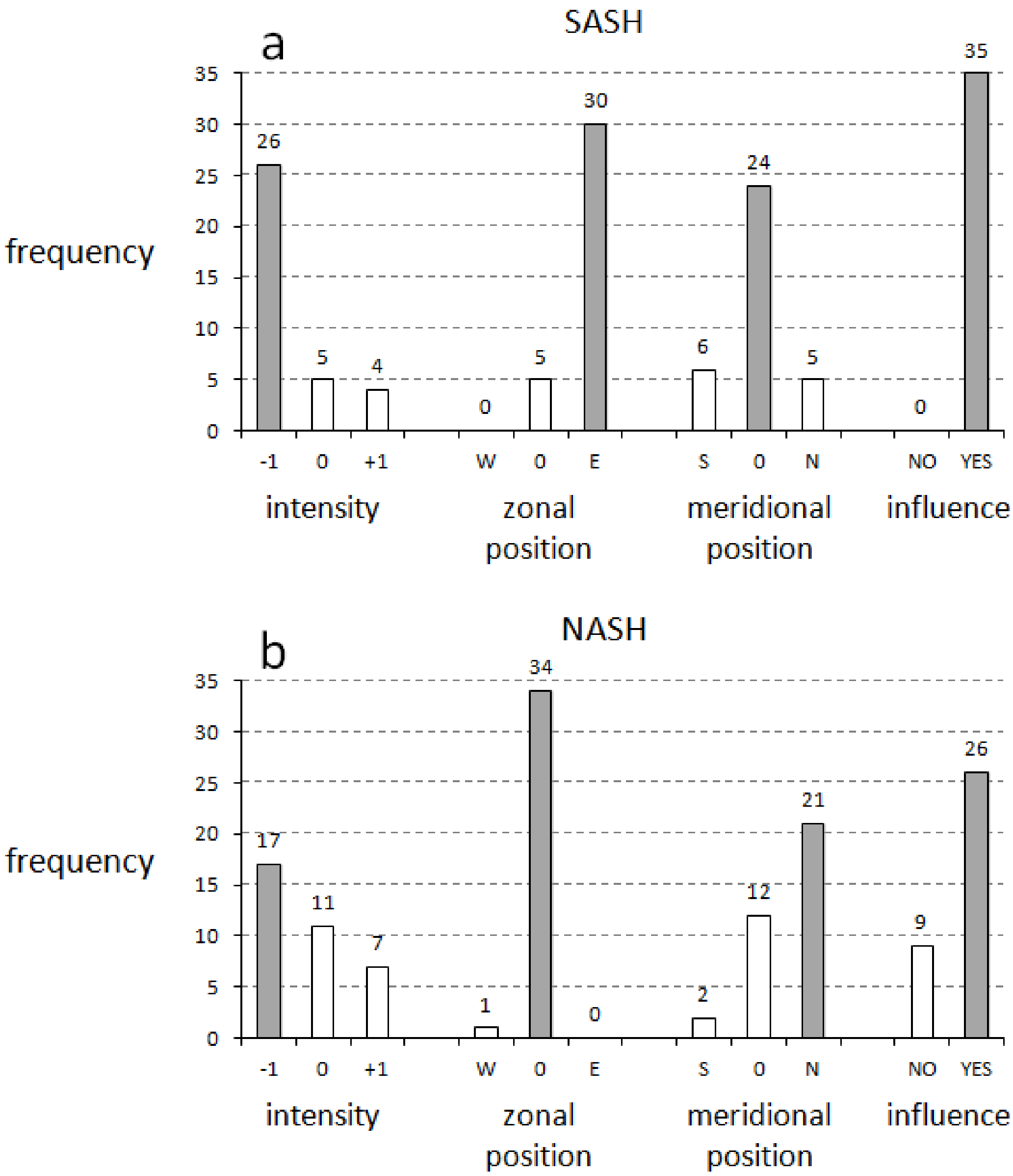

Fig. 11 For SASH (a) and NASH (b), frequency of categories – intensity (+1: intensification, 0: no change, -1: weakening) zonal position (W: westward displacement, 0: no change, E: eastward displacement), meridional position (S: southward displacement, 0: no change, N: northward displacement) and influence (YES: the is influence, NO: there is no influence) – in the transition from VMAX to VMIN. For SASH, influence means weakening or eastward propagation in the transition; for NASH, weakening or northward propagation. In each category, gray bar refers to the highest frequency.

6. Discussion

The connection between SASH and surface wind in NEB is well known, particularly for longer temporal scales (e.g. intraseasonal and interannual) [32, 37]. For instance, Degola (2013) [38] showed that when SASH is displaced westward (eastward) from its climatological position, more (less) intense winds occur over NEB. Recently, Gilliand and Keim (2018) showed that this relation also holds for shorter temporal scales, such as the daily scale. Therefore, the influence of the zonal position of SASH on C5d phases obtained here agrees with previous studies. The contribution of the present study consists of showing that the intensity of SASH and NASH, as well as the meridional position of NASH, are additional factors that influence C5d phases.

In previous studies that identify C5d in NEB, such as Marciotto et al. (2012) [13] for CLA and Moura et al. (2014) [18] for a locality in the eastern coast of Brazil, SASH (or NASH) was not mentioned as a possible driver of C5d. The reason might be the idea that C5d would result from the direct action of an atmospheric system over NEB. Results obtained here show that the influence is mostly indirect: for instance (limiting the discussion to SASH), frontal systems affect SASH, which in turn affects the southeast trades that reach the northern coast of NEB. Therefore, the frequent occurrence of C5d in CLA during the dry quarter is not related to the infrequent direct influence of frontal systems on CLA [26], but to the frequent influence of frontal systems on SASH.

Ito (1999) [39] showed that daily changes of SASH position reveal a periodicity similar to that of frontal systems. Therefore, the frequency of frontal systems occurrence could explain the period of C5d, which is about 5-6 days. For the dry quarter, Pampuch and Ambrizzi (2015) [40] showed that the mean time interval between the passage of successive frontal systems over Southern Brazil is 6-8 days. This interval is similar to the period of C5d and explains the occurrence of peaks in the 6-9 days band in the global wavelet spectrum (Fig. 3). However, since there are also peaks at periods < 6 days (such as 4 days), other factors affect the period of C5d. Further studies are necessary to unravel these factors.

Results were obtained addressing the transition from VMAX to VMIN. How is VMAX established from VMIN? Focusing only on the Southern Hemisphere, the question means how an intense SASH extending over the South Atlantic could follow VMIN. As a frontal system propagates, the trough that separates SASH from the migratory anticyclone gradually weakens (as illustrated by comparing Fig. 9f with Fig. 9h). When it disappears, SASH and the migratory anticyclone merges, which results in the expansion of SASH over the South Atlantic. It gives rise to VMAX. Merging between the migratory anticyclone and SASH after the frontal system passage, which is the key process to the establishment of VMAX, is well known [41, 42].

One observational feature obtained here was the more pronounced counterclockwise rotation of the surface circulation over the northern coast of NEB in VMIN. For cases when the counterclockwise rotation is even more pronounced, northerly winds can occur at CLA and this high rotation can be related to the formation of a low-level mesoscale anticyclone over NEB. One such case occurred from 23 to 25-Nov-1999 during the launch operation called *Operação Almenara* and was reported by Marques (2004) [25].

7. Concluding Remarks

The main features of C5d during the dry quarter in CLA were obtained from observed data over the course of 9 years. The cycle consists of a variability in the 3-9 days band concentrated around the period of 5 days. C5d occurs frequently and its active periods occur in about 1/3 of dry quarter days. There is large interannual variability of C5d activity. The distribution of wind speed and direction for C5d phases shows that, from VMAX to VMIN, the surface wind over CLA weakens (reduction from 9-12 m/s to 9-6 m/s) and rotates counterclockwise (from ENE to NE direction).

To obtain the distinct features between the C5d phases, 35 cases subjectively sampled to represent typical cases of C5d during active periods were analyzed. Results showed that, from VMAX to VMIN, SASH weakens or propagates eastwards for all cases, while NASH weakens or propagates northwards for about 3/4 of cases. Therefore, SASH could be regarded as the main driver of C5d, while NASH could be considered as an important complementary forcing of C5d.

Previous studies [39] showed that the southwesterly propagation of frontal systems over South America drives the zonal displacement of SASH. The frontal system trough pushes SASH eastwards, and this displacement leads to wind velocity reduction in CLA (VMIN). Behind the trough, the migratory anticyclone intensifies and, after the trough weakening and dissipation, merges with the SASH [41]. Expansion of SASH over South Atlantic due to this merging process results in wind velocity increase in CLA (VMAX). The cycle is repeated when a new frontal system comes up. This conceptual model integrates aspects obtained in this study and could be useful for short-range wind forecasting during launch operations at CLA.

Acknowledgements

This work is part of the first author's MSc dissertation under the guidance of the second author. The authors wish to thank the dissertation committee members, Dr. Gilberto Fernando Fisch, Dr. Arcilan Trevenzoli Assireu and Dr. Renato Galante Negri, for their comments and suggestions.

References

[1] I. Pereira, G. F. Fisch, I. Miranda, L. A. T. Machado and M. A. S. Alves, Atlas climatológico do Centro de Lançamento de Alcântara. Instituto de Aeronáutica e Espaço, technical report, 2002.

[2] S. S. Barros, Precipitação no Centro de Lançamento de Alcântara: aspectos observacionais e de modelagem, MSc dissertation, Instituto Nacional de Pesquisas Espaciais, São José dos Campos, 2008.

[3] E. R. Marciotto and G. Fisch, Investigation of approaching ocean flow and its interaction with land internal boundary layer, *American Journal of Environmental Engineering* 3 (2013) (1) 18-23.

[4] P. C. S. Costa, M. D. Oyama and R. F. C. Marques, Wet days in the dry quarter of the Alcântara Launch Center Region: Observational features, *Journal of Aerospace Technology and Management* 11 (2019) e3219.

[5] J. Kingwell, J. Shimizu, K. Narita, H. Kawabata and Shimizu, Weather factors affecting rocket operations: A review and case history, *Bulletin of the American Meteorological Society* 72 (1991) (6) 778-794.

[6] L. E. Medeiros, R. O. Magnago, G. Fisch and E. R. Marciotto, Observational study of the surface layer at an ocean-land transition region, *Journal of Aerospace Technology and Management* 5 (2013) (4) 449-458.

[7] D. Schuch and G. Fisch, The use of an atmospheric model to simulate the rocket exhaust effluents transport and dispersion for the Centro de Lançamento de Alcântara, *Journal of Aerospace Technology and Management* 9 (2017) (2) 137-146.

[8] A. C. Avelar, F. L. C. Brasileiro, A. G. Marto, E. R. Marciotto, G. Fisch and A. F. Faria, Wind tunnel simulation of the atmospheric boundary layer for studying the wind pattern at Centro de Lançamento de Alcântara, *Journal of Aerospace Technology and Management* 4 (2012) (4) 463-473.

[9] A. F. G. Silva and G. Fisch, Avaliação do Modelo WRF para a Previsão do Perfil do Vento no Centro de Lançamento de Alcântara, *Revista Brasileira de Meteorologia* 29 (2014) (2) 259-270.

[10] A. S. Souza, Condições Atmosféricas durante a Operação Raposa. São José dos Campos: Instituto de Aeronáutica e Espaço, Technical Report, 2014.

[11] D. M. Custódio, V. M. Couto, J. Yamasaki and G. F. Fisch, Uso do Weather Research and Forecasting na Previsão de Velocidade do Vento no Centro de Lançamento de Alcântara, in: *Proceedings of the X Workshop Brasileiro de Micrometeorologia*, Santa Maria, Brazil, 2017.

[12] A. S. Souza, Condições Atmosféricas durante a Operação Iguaíba, São José dos Campos: Instituto de Aeronáutica e Espaço, Technical Report, 2013.

[13] E. R. Marciotto, Fisch Gilberto and L. E. Medeiros, Characterization of surface level wind in the Centro de Lançamento de Alcântara for use in rocket structure loading and dispersion studies, *Journal of Aerospace Technology and Management* 4 (2012) (1) 69-79.

[14] E. D. J. Reuter, Sensibilidade do modelo MM5 no prognóstico do vento às diferentes parametrizações de Camada Limite Planetária no Centro de Lançamento de Alcântara, PhD thesis, Instituto Nacional de Pesquisas Espaciais, São José dos Campos, 2013.

[15] I. V. D. Hoven, Power spectrum of horizontal wind speed in the frequency range from 0.0007 to 900 cycles per hour, *Journal of Meteorology* 14 (1957) (2) 160-164.

[16] H. J. Hwang, Power density spectrum of surface wind speed on Palmyra Island, *Monthly Weather Review* 98 (1970) (1) 70-74.

[17] Y. Mori, A study on climatological aspects of winds in Japan, Part I: Mean wind fields and annual variations of winds, *Journal of Climate* 1 (1988) (2) 132-142.

[18] M. Moura and R. Carneiro, Estudo dos padrões climatológicos do vento usando transformada em ondeletas, *Revista Brasileira de Geografia Física* 7 (2014) (5) 774-782.

[19] A. Diedhiou, L. A. T. Machado and H. Laurent, Mean kinematic characteristics of synoptic easterly disturbances over the Atlantic, *Advances in Atmospheric Sciences* 27 (2010) (3) 483-499.

[20] R. R. Torres and N. J. Ferreira, Case studies of easterly wave disturbances over Northeast Brazil using the eta model, *Weather and Forecasting* 26 (2011) (2) 225-235.

[21] L. C. B. Molion and S. O. Bernardo, Uma revisão da dinâmica das chuvas no Nordeste brasileiro, *Revista Brasileira de Meteorologia* 17 (2002) (1) 1-10.

[22] R. R. Chaves and I. F. Cavalcanti, Atmospheric circulation features associated with rainfall variability over Southern Northeast Brazil, *Monthly Weather Review* 129 (2001) (10) 2614-2626.

[23] E. C. Coutinho and G. Fisch, Distúrbios Ondulatórios de Leste (DOLs) na Região do Centro de Lançamento de Alcântara-MA, *Revista Brasileira de Meteorologia* 22 (2007) (2) 193-203.

[24] R. F. C. Marques, M. A. S. Alves and M. D. Oyama, Variabilidade do Vento na Escala de 3-9 Dias sobre Alcântara e Natal, in: *Proceedings of the III Simpósio Internacional de Climatologia*, Canela, Brazil, 2009.

[25] R. F. C. Marques, Influência de Sistemas Meteorológicos no Regime de Vento no Centro de Lançamento de Alcântara (CLA), in: *Proceedings of the XIII Congresso Brasileiro de Meteorologia*, Fortaleza, Brazil, 2004.

[26] P. S. Tavares, Um estudo observacional da incursão de sistemas frontais no nordeste brasileiro e sua influência na atmosfera do Centro de Lançamento de Alcântara (CLA), MSc dissertation, Instituto Nacional de Pesquisas Espaciais, São José dos Campos, 2008.

[27] C. Torrence and G. P. Compo, A practical guide to wavelet analysis, *Bulletin of the American Meteorological Society* 79 (1998) (1) 61-78.

[28] R. F. C. Marques and G. F. Fisch, As atividades de Meteorologia Aeroespacial no Centro Técnico Aeroespacial (CTA), *Boletim da Sociedade Brasileira de Meteorologia* 29 (2005) (3) 21-26.

[29] D. P. Dee, S. M. Uppala, A. J. Simmons, P. Berrisford, P. Poli, S. Kobayashi, U. Andrae, M. A. Balmaseda, G. Balsamo and P. Bauer et al., The ERA-Interim reanalysis: configuration and performance of the data assimilation system, *Quarterly Journal of the Royal Meteorological Society* 137 (2011) (656) 553-597.

[30] C. A. F. Gisler, G. Fisch and C. S. Correa, Análise estatística do perfil de vento na camada limite superficial no centro de lançamento de Alcântara, *Journal of Aerospace Technology and Management* 3 (2011) (2) 193-202.

[31] K. A. C. Ramalho, Ciclo de 5 dias do vento em baixos níveis durante o trimestre seco do Centro de Lançamento de Alcântara, MSc dissertation. Instituto Nacional de Pesquisas Espaciais, São José dos Campos, 2018.

[32] M. S. Reboita, T. Ambrizzi, B. A. Silva, R. F. Pinheiro and R. P. Rocha, The South Atlantic subtropical anticyclone: Present and future climate, *Frontiers in Earth Science* 7 (2019) Article 8.

[33] Climanálise, *Boletim de Monitoramento e Análise Climática* 28 (2013) 11, Instituto Nacional de Pesquisas Espaciais, Centro de Previsão do Tempo e Estudos Climáticos.

[34] R. E. Davis, B. P. Hayden, D. A. Gay, W. L. Phillips and G. V. Jones, The North Atlantic subtropical anticyclone, *Journal of Climate* 10 (1997) (4) 728-744.

[35] J. W. Hurrel and C. Deser, North Atlantic climate variability: The role of the North Atlantic Oscillation, *Journal of Marine Systems* 78 (2009) (1) 28-41.

[36] C. W. Landsea and E. S. Blake, Hurricane Humberto, National Oceanic and Atmospheric Administration, National Hurricane Center Tropical Cyclone Report, 2014.

[37] X. Sun, K. H. Cook and E. K. Vizy, The South Atlantic Subtropical High: Climatology and interannual variability, *Journal of Climate* 30 (2017) (9) 3279-3296.

[38] T. S. D. Degola, Impactos e variabilidade do anticiclone subtropical do Atlântico Sul sobre o Brasil no clima presente e em cenários futuros, MSc dissertation, Universidade de São Paulo, São Paulo, 2013.

[39] E. R. K. Ito, Um estudo climatológico do anticiclone subtropical do Atlântico Sul e sua influência em sistemas frontais, MSc dissertation. Universidade de São Paulo, São Paulo, 1999.

[40] L. A. Pampuch and T. Ambrizzi, Sistemas Frontais sobre a América do Sul Parte I: Climatologia e intervalo de passagem em dados da Reanálise I do NCEP/NCAR, in: *Proceedings of the IX Workshop Brasileiro de Micrometeorologia*, Santa Maria, Brazil, 2015.

[41] P. Satyamurty, C. A. Nobre and P. L. Silva Dias, South America, in: Karoly D. J., Vincent D. G. (Eds.), *Meteorology of the Southern Hemisphere: Meteorological Monographs*, American Meteorological Society, Boston, MA. 1998.

[42] M. L. G. Rodrigues, D. Franco and S. Sugahara, Climatologia de Frentes Frias no Litoral de Santa Catarina, *Revista Brasileira de Geografia Física* 22 (2004) (2) 135-151.